A Small Variation in Weather Conditions Could Lead to Dramatic Changes of Dengue Outbreaks

Supplementary Information

Lengyang Wang[1], Ruiyun Li[2], Alex R. Cook[3], Shengjie Lai[4], Nils Chr. Stenseth[2], Howell Tong[5], and Yingcun Xia[1]

[1]Department of Statistics and Data Science, National University of Singapore, Singapore 117546
[2]Centre for Ecological and Evolutionary Synthesis, Department of Biosciences, University of Oslo, N-0316 Oslo, Norway
[3]Saw Swee Hock School of Public Health, National University of Singapore and National University Health System, Singapore 117549
[4]School of Geography and Environmental Science, University of Southampton, Southampton SO17 1BJ, United Kingdom
[5]Department of Statistics, London School of Economics and Political Science, London WC2A 2AE, United Kingdom

Contents

1 Data

The data used in our analysis are the reported dengue cases in Thailand (the Center of Epidemiological Information, Bureau of Epidemiology, Ministry of Public Health https://apps.doe.moph.go.th/boeeng/about_us.php), Singapore (The National Environment Agency, https://www.nea.gov.sg/) and South America countries (The Pan American Health Organization, https://www.paho.org/en). For the weather conditions (precipitation and temperature), the data are obtained from the National Centers for Environmental Information (NCEI, https://www.ncei.noaa.gov/). Air-pollution data are only available to Southeast Asian countries and they come from Air Quality Historical Data Platform https://aqicn.org/data-platform/register/. However, except for Singapore, for most regions in Southeast Asia and South America, the precipitation data are not complete. So, we use the overall mean value to replace the missing values of precipitation. We use the data from 2014 to 2020 as the data in the period are available for all regions. The climate and air-pollution data are daily and dengue cases for Singapore and South America countries are weekly. The dengue cases for Thailand are monthly, and we transform them into weekly cases for the models and simulations. For GAI index, the data is available online [1] and its time span is from January 2014 to September 2016. Because symptoms of dengue fever are similar to flu-like diseases and for other reasons, dengue fevers are commonly regarded as influenza or diseases other than dengue fevers.

Thus dengue cases are grossly under-reported. The under-reporting rate can be as high as 2500%. The rates differ for different countries. Table 1 shows the under-reporting rates for different countries. It is interesting to see that the reporting rate in 2020 in Singapore is much lower because more people did the test due to their concern with COVID-19. We corrected the dengue case according to the under-reporting rates for our data analysis.

Table 1: **Country and under-reporting rates**

Country	under-reporting rate	references
Singapore	14 from 2005 to 2009 6 from 2014 to 2017 3 in 2020	[2] (personal communication with MOH of Singapore)
Thailand	7	[3]
South America	25.1	[4]

2 Simulation based on TSIR

Without considering weather conditions, we fit model (2.3) in the main context using the data of Singapore; the simulated dynamics is shown in the Fig. 1(A). The dynamics significantly differs from the observed numbers of cases, indicating possible omission of some important factors. For example, residuals between observed numbers and the fitted dynamics have clear dependence on both temperature and precipitation in the past days as shown in Fig. 1(B) and (C), leading to our ETSIR(S) model.

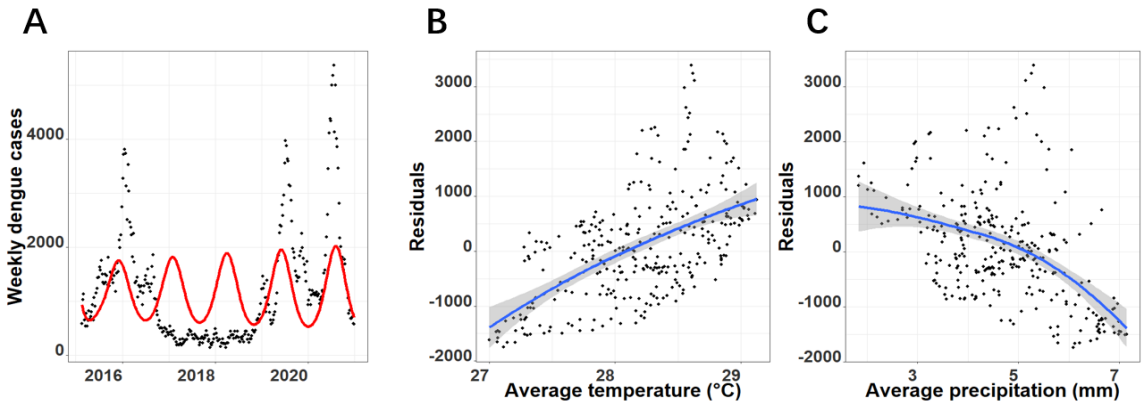

Figure 1: **Simulated dynamics and the dependence between its residuals with weather conditions.** **[A]Simulated dynamics, I_t, based on model (2.3) in the main context (red-curve), and observed numbers of cases (dots), I_t.** **[B]Plots of residuals $(I_t - \hat{I}_t)$ against average temperature.** **[C]Plots of residuals $(I_t - \hat{I}_t)$ against average precipitation. The averages are defined as $\sum_{k=1}^{K_T} T_{t-k}/K_T$ and $\sum_{k=1}^{K_P} P_{t-k}/K_P$, where $K_P = 180$ days and $K_T = 140$ days.**

3 ETSIR(S) model with air-pollutants

Following the discussion in section **Models and estimations** in the main context, a general ETSIR(S) model with both pollutants and weather conditions is:

$$\begin{aligned} E(I_t) =& \{c_0 + c_I \times \sum_{k=1}^{K_I} I_{t-k} + \mathrm{g}_P(\sum_{k=1}^{K_P} P_{t-k}/K_P) + \mathrm{g}_T(\sum_{k=1}^{K_T} T_{t-k}/K_T) \\ &+ c_M \times \sum_{k=1}^{K_M} M_{t-k}/K_M + c_O \times \sum_{k=1}^{K_O} O_{t-k}/K_O + c_N \times \sum_{k=1}^{K_N} N_{t-k}/K_N\} \times I_{t-1}, \end{aligned} \tag{1}$$

where M is the daily PM_{10}, O is the daily O_3, N is the daily NO_2, P is the daily average precipitation, H_P is the threshold of the daily average of precipitation, T is the daily average temperature and H_T is the threshold of the daily average of temperature. K_I is the number of days for the accumulation of infected people and K_P, K_T, K_M, K_O, K_N are the number of days for the accumulation of pollutants and weather factors. $\mathrm{g}_P(v) = c_P \times v + c'_P \times (v - H_P) \times I(v - H_P > 0)$ and $\mathrm{g}_T(v) = c_T \times v + c'_T \times (v - H_T) \times I(v - H_T > 0)$,

respectively. These functions are employed to model the possible changing points for the effect of precipitations and temperature in different levels. For pollutants, we simply model the effect linearly.

4 Model estimation and statistical inference

To make statistical inference about the model, we re-sample [5] data by the following model based on the estimated parameters.

$$\begin{aligned} I_t^* &= \{\hat{c}_0 + \hat{c}_I \sum_{k=1}^{\hat{K}_I} I_{t-k}^* + \hat{\mathrm{g}}_P(\sum_{k=1}^{\hat{K}_P} P_{t-k}/\hat{K}_P) + \hat{\mathrm{g}}_T(\sum_{k=1}^{\hat{K}_T} T_{t-k}/\hat{K}_T) + \hat{c}_M \sum_{k=1}^{\hat{K}_M} M_{t-k}/\hat{K}_M \quad (2) \\ &+ \hat{c}_O \sum_{k=1}^{\hat{K}_O} O_{t-k}/\hat{K}_O + \hat{c}_N \sum_{k=1}^{\hat{K}_N} N_{t-k}/\hat{K}_N\} \times I_{t-1}^* + \epsilon_t^* \times \hat{e}_t, \end{aligned}$$

where ϵ_t^* follows the standard normal distribution and $\hat{e}_t = I_t - \hat{I}_t$ is the residual of the observed data and the fitted dynamics. To make inference about the model, we run simulation B times and thus get B time series of cases. For each of the B time series, we estimate the model again, and denote the estimators by $c_0^{*i}, c_I^{*i}, c_P^{*i}, c_P^{'*i}, c_T^{*i}, c_T^{'*i}, c_M^{*i}, c_O^{*i}, c_N^{*i}, i = 1, ..., B$. Under some regularity conditions [5], it can be shown that the empirical distribution of $\{c_0^{*i}, c_I^{*i}, c_P^{*i}, c_P^{'*i}, c_T^{*i}, c_T^{'*i}, c_M^{*i}, c_O^{*i}, c_N^{*i}, i = 1, ..., B\}$ approximates the distribution of $\hat{c}_0, \hat{c}_I, \hat{c}_P, \hat{c}_P^{'}, \hat{c}_T, \hat{c}_T^{'}, \hat{c}_M, \hat{c}_O, \hat{c}_N$. Thus, we can calculate the $p-$values for testing whether these coefficients are zero or not. For example, to test $H_I^0 : c_I = 0$ the p-value is calculated as follows

$$pval_I = \frac{\#\{\hat{c}_I \times c_I^{*i} \leq 0, i = 1, ..., B\}}{B}.$$

In this estimation, we keep $K_I, ..., K_N$ fixed because its estimator is almost fixed in the resampling. With $B = 2000$, the approximated p-values are shown in Table 2 and 3.

Table 2: **Estimated parameters for all regions/countries considering temperature and precipitation. [1]Values on top are the regression coefficients. [2]Values in the bracket are the corresponding p-values based on re-sample method (3).**

	Countries					
coefficients	Costa Rica	Dominican Republic	Paraguay	Colombia	Bolivia	Honduras
c_0	-4.19 (5.00×10^{-4})	-2.39 (0)	6.66 (1.50×10^{-3})	-1.27 (1.50×10^{-3})	2.57 (8.50×10^{-3})	3.04 (1.00×10^{-3})
c_I	-4.41×10^{-7} (0)	-1.13×10^{-6} (0)	-1.36×10^{-7} (0)	-4.90×10^{-8} (3.00×10^{-1})	-2.36×10^{-7} (5.00×10^{-4})	-2.76×10^{-7} (2.50×10^{-3})
c_P	1.85×10^{-2} (6.50×10^{-2})	-1.02×10^{-1} (1.25×10^{-3})	-4.01×10^{-1} (9.15×10^{-2})	2.48×10^{-2} (4.98×10^{-2})	-2.29×10^{-1} (7.15×10^{-2})	-2.19×10^{-1} (4.50×10^{-3})
c'_P	-1.02×10^{-1} (2.20×10^{-2})	6.41×10^{-2} (1.01×10^{-2})	3.27×10^{-1} (3.14×10^{-2})	-5.83×10^{-2} (1.85×10^{-2})	4.30×10^{-1} (2.48×10^{-2})	2.04×10^{-1} (2.05×10^{-2})
c_T	2.27×10^{-1} (1.50×10^{-2})	1.49×10^{-1} (5.50×10^{-2})	-6.22×10^{-2} (3.42×10^{-1})	1.30×10^{-1} (5.55×10^{-3})	4.10×10^{-4} (3.53×10^{-1})	-4.76×10^{-2} (2.36×10^{-2})
c'_T	-1.39×10^{-1} (1.75×10^{-2})	-4.68×10^{-2} (1.39×10^{-1})	3.92×10^{-1} (3.33×10^{-2})	-1.71×10^{-1} (2.50×10^{-2})	1.71×10^{-1} (8.18×10^{-2})	-3.49×10^{-2} (1.22×10^{-1})
H_P	8.04	5.32	10.53	6.15	7.85	3.30
H_T	22.50	27.13	26.49	16.77	23.71	27.77
K_I	161	203	196	35	182	84
K_P	146	45	166	170	64	151
K_T	172	119	108	179	86	149
coefficients	Mexico	Singapore	Bangkok	Chiangmai	Chonburi	Nakhon Sawan
c_0	7.89×10^{-1} (1.50×10^{-3})	-1.73 (0)	-5.79 (0)	-8.23×10^{-1} (5.00×10^{-4})	-1.68 (5.00×10^{-4})	6.48×10^{-1} (5.00×10^{-4})
c_I	-7.70×10^{-8} (0)	-3.02×10^{-6} (0)	-7.14×10^{-6} (5.00×10^{-4})	-1.99×10^{-5} (8.50×10^{-3})	-2.08×10^{-5} (1.00×10^{-4})	-2.41×10^{-5} (0)
c_P	7.17×10^{-2} (4.50×10^{-3})	4.48×10^{-2} (4.60×10^{-2})	1.40×10^{-1} (1.75×10^{-2})	6.66×10^{-2} (3.52×10^{-2})	1.46×10^{-1} (4.10×10^{-2})	7.03×10^{-3} (2.95×10^{-1})
c'_P	-4.95×10^{-2} (5.85×10^{-3})	-3.32×10^{-1} (1.20×10^{-2})	-1.71×10^{-1} (1.35×10^{-2})	-2.08×10^{-1} (2.75×10^{-2})	-2.39×10^{-1} (9.00×10^{-3})	-4.53×10^{-2} (8.60×10^{-2})
c_T	1.12×10^{-2} (1.10×10^{-2})	9.67×10^{-2} (9.50×10^{-3})	1.94×10^{-1} (9.95×10^{-3})	5.79×10^{-2} (1.85×10^{-2})	6.03×10^{-2} (7.30×10^{-3})	1.66×10^{-2} (3.85×10^{-2})
c'_T	6.32×10^{-2} (3.35×10^{-2})	-8.36×10^{-2} (7.10×10^{-2})	-1.78×10^{-1} (1.45×10^{-2})	-1.41×10^{-2} (3.11×10^{-1})	-7.82×10^{-2} (1.40×10^{-2})	-2.18×10^{-2} (8.88×10^{-2})
H_P	1.67	5.61	10.04	6.91	7.88	6.04
H_T	18.32	27.98	29.28	27.90	28.68	29.73
K_I	112	203	210	105	196	175
K_P	45	149	93	152	178	133
K_T	163	131	167	115	129	127

Table 3: **Estimated parameters in the models of Bangkok, Singapore, Chiangmai, Nakhon Sawan and Chonburi considering all climate factors. [1]Values on top are the regression coefficients. [2]Values in the bracket are the corresponding p-values based on re-sample method (3).**

	Singapore	Bangkok	Chiangmai	Chonburi	Nakhon Sawan
c_0	-3.12 (0)	-9.87×10^{-2} (0)	4.79×10^{-2} (0)	-2.54 (0)	1.17×10^{1} (0)
c_M	2.00×10^{-4} (6.55×10^{-2})	-6.27×10^{-3} (1.80×10^{-2})	-1.42×10^{-3} (9.80×10^{-2})	5.22×10^{-3} (5.34×10^{-2})	6.69×10^{-3} (2.25×10^{-2})
c_O	1.95×10^{-2} (1.40×10^{-2})	9.30×10^{-3} (4.50×10^{-3})	5.92×10^{-3} (6.25×10^{-2})	-8.22×10^{-3} (2.10×10^{-2})	1.27×10^{-2} (1.85×10^{-2})
c_N	6.64×10^{-3} (2.71×10^{-2})	-1.45×10^{-2} (3.50×10^{-2})	-3.15×10^{-3} (3.07×10^{-1})	1.51×10^{-2} (0)	-1.00×10^{-1} (5.40×10^{-3})
c_P	4.03×10^{-2} (6.55×10^{-3})	2.32×10^{-2} (2.30×10^{-2})	4.24×10^{-4} (4.31×10^{-1})	1.81×10^{-1} (0)	-2.49×10^{-2} (1.05×10^{-2})
c'_P	-6.74×10^{-2} (1.55×10^{-2})	-3.99×10^{-2} (6.00×10^{-2})	-3.65×10^{-3} (1.53×10^{-1})	-2.67×10^{-1} (1.25×10^{-2})	-1.80×10^{-2} (1.51×10^{-1})
c_T	1.25×10^{-1} (0)	4.39×10^{-2} (3.15×10^{-3})	3.73×10^{-2} (0)	7.52×10^{-2} (0)	-3.64×10^{-1} (2.15×10^{-2})
c'_T	-9.35×10^{-2} (6.00×10^{-3})	-1.89×10^{-3} (4.20×10^{-1})	-3.42×10^{-2} (1.72×10^{-3})	-1.71×10^{-2} (2.28×10^{-2})	4.24×10^{-1} (0)
c_I	-2.20×10^{-6} (0)	-6.60×10^{-6} (0)	-8.87×10^{-6} (2.40×10^{-3})	-1.60×10^{-5} (7.50×10^{-3})	-6.48×10^{-6} (3.00×10^{-2})
H_P	5.32	11.30	6.01	7.81	6.53
H_T	28.24	28.74	27.70	28.50	28.72
K_I	119	210	126	196	133
K_M	23	124	19	168	129
K_O	148	20	87	142	91
K_N	124	178	125	39	110
K_P	169	45	38	155	143
K_T	58	106	25	120	178

5 Other simulations based on fitted models (1)

Both deterministic realization and random stochastic realization are simulated for the fitted model (1). For the former, the dynamics considering only temperature and precipitation is generated in the main context, while the dynamics considering all environmental factors is generated from (1). For the latter, the random noise (based on the residuals) is used and the dynamics is generated by (3). For all regions, deterministic realizations of the models are shown in Fig. 2 in the main context, Fig. 2 (considering only precipitation and temperature) and Fig. 3 (Southeast Asian regions considering all environmental factors); while those with random noises are shown in Fig. 4. It is interesting to see that, except for Singapore, adding air-pollution variables does not improve the simulated dynamics significantly in terms of fitting accuracy. This may imply that the impact of air-pollutant on the transmission is negligible in most regions [6, 7].

In Fig. 2, the fitted dynamics of Chonburi has much higher peaks than the observed data. Note that when some unpredictable event occurs that is not modelled, the dynamics may differ substantially from the simulated dynamics and this event also has impact on the later dynamics. To further show our model's ability to model the latter effect of those events, we start our simulation after the event. Taking Chonburi as an example, we choose the start point in 2016 and run the simulation again using the same parameters. The corresponding simulated dynamics (blue solid lines) can indeed give a more accurate fit compared to the original one (red solid lines). Since most of the simulated dynamics are very close to the observed ones, this again provides evidence that a fitted ETSIR(S) model can capture the main dynamics of transmission. It's also observed that the temperature plays the most significant role in the dynamics. However, the other factors can also affect the dynamics on their own and may be different for different cities, and in different ways.

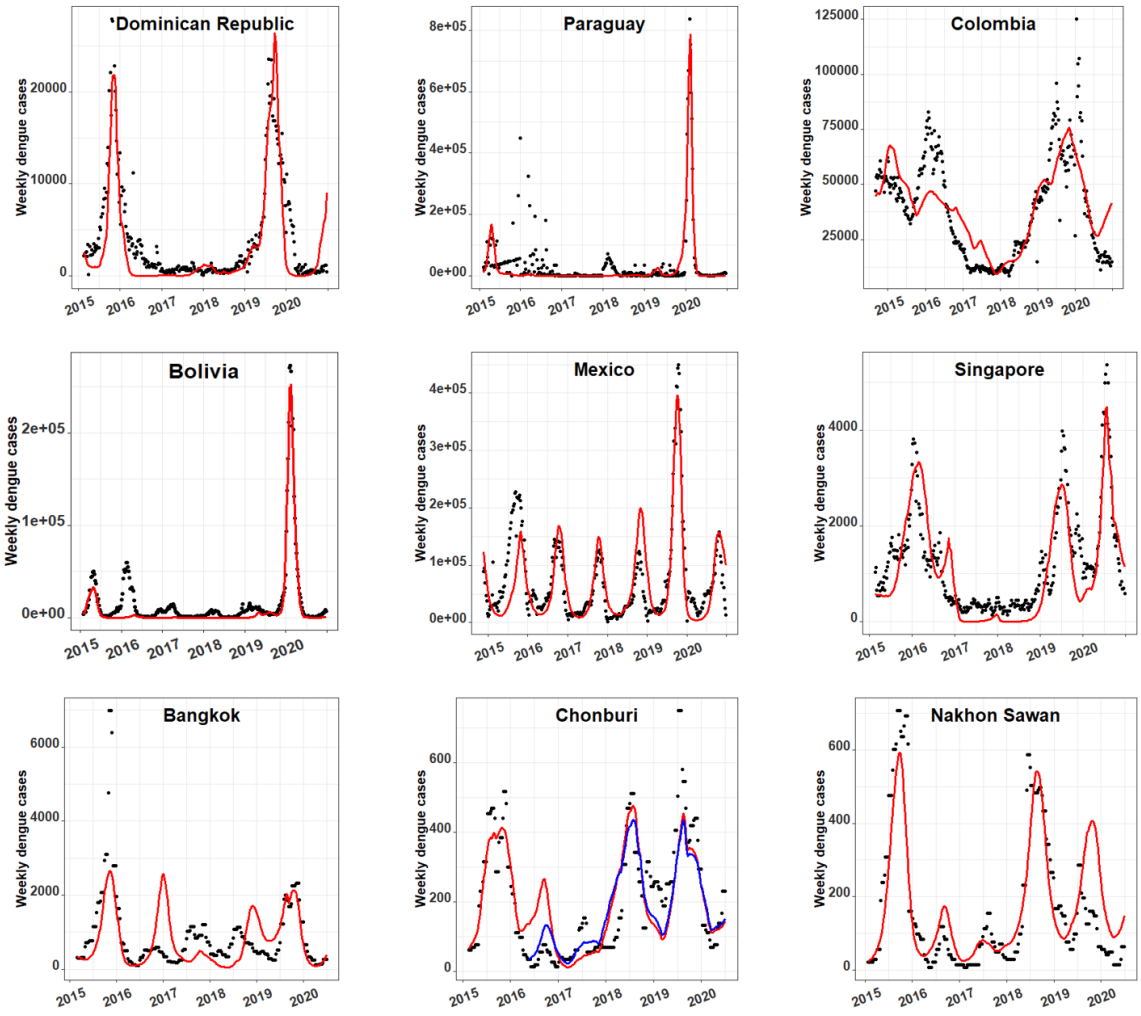

Figure 2: **Simulation dynamics 1 (fitting with precipitation and temperature). [1]Black dots: real weekly dengue cases. [2]Red solid lines: simulated weekly dengue cases. [3]Blue solid lines: simulated weekly dengue cases with a new start point.**

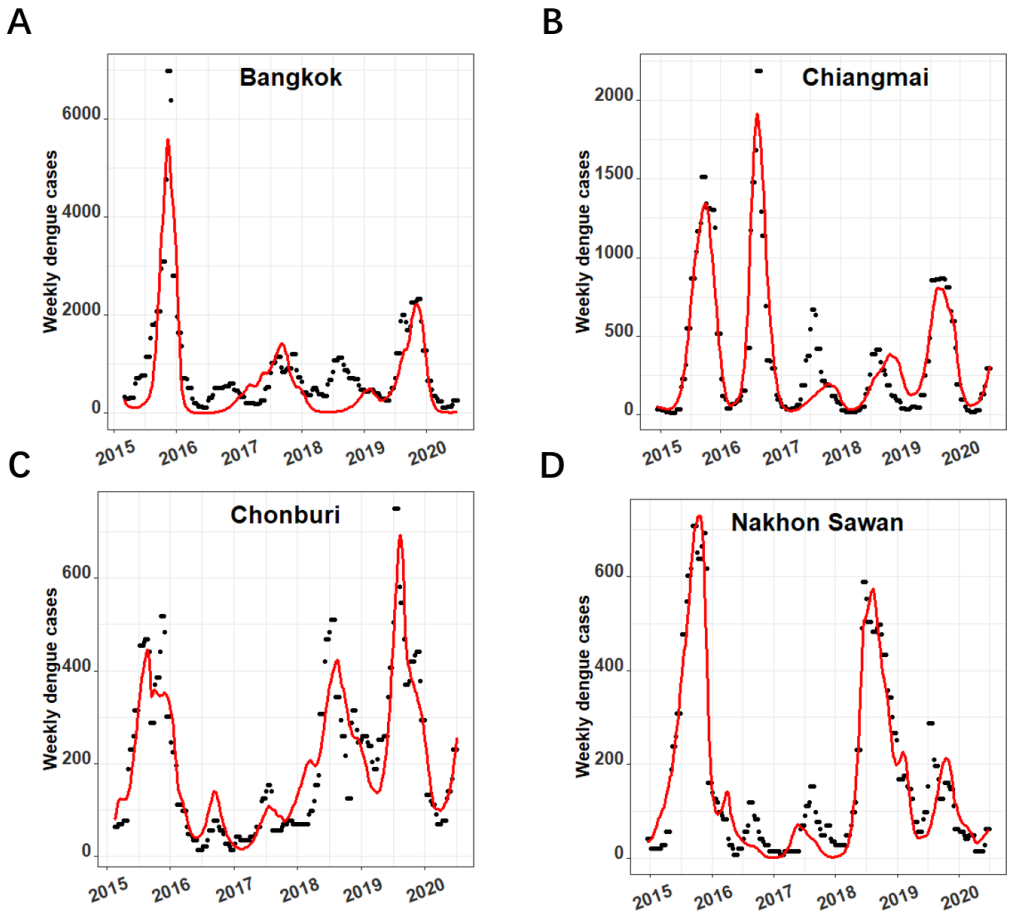

Figure 3: **Simulation dynamics 2 (fitting with all climate factors) based on (1). [1]Black dots: real weekly dengue cases. [2]Red solid lines: simulated weekly dengue cases.**

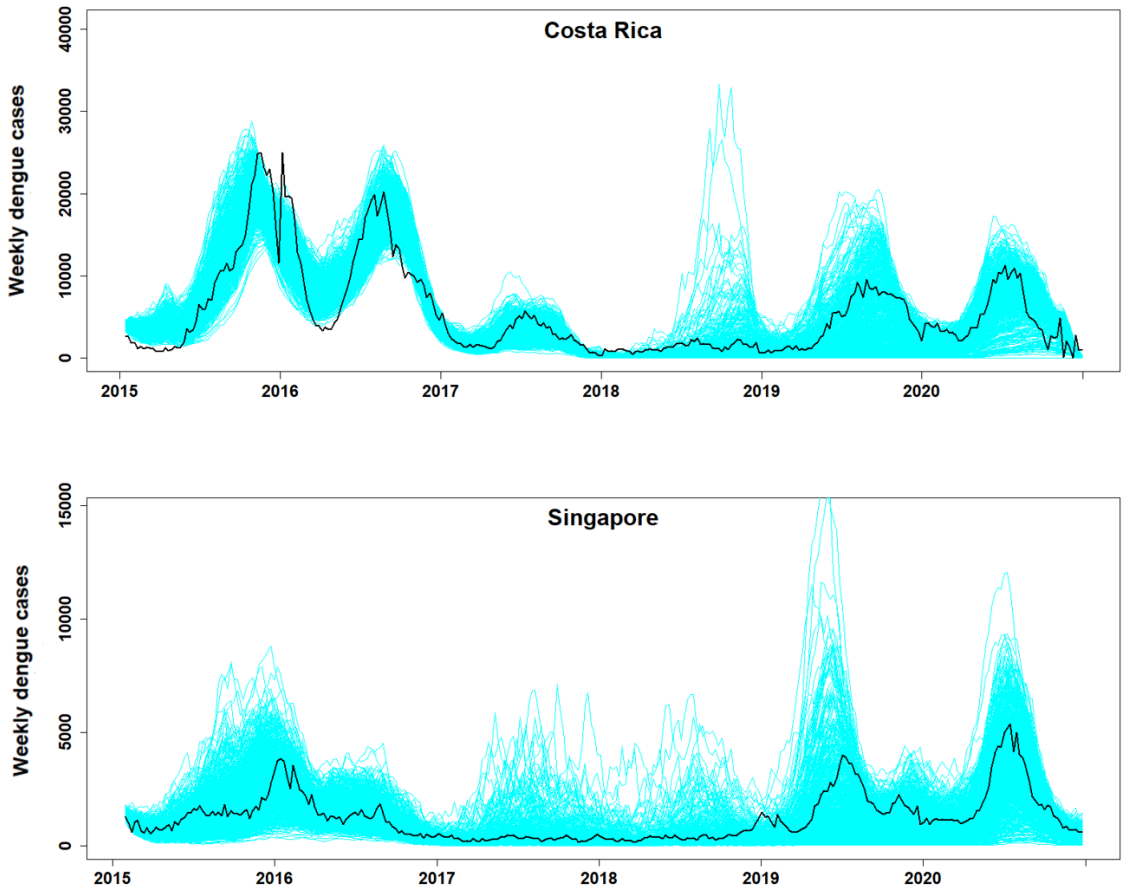

Figure 4: **Simulation dynamics of Costa Rica and Singapore with random noise based on (3). [1]Black solid lines: observed weekly dengue cases. [2]Cyan shaded area: simulated weekly dengue cases with random noise.**

6 Model prediction

Originally, our models in this study were fitted to the end of 2020. Now, data in 2021 are available (with many missing values in the data for South America regions). As a result, we can use the estimated model to predict the data in 2021. As shown in the Fig. 5, even

with possible bigger underreporting rates and changes of prevention policy due to COVID-19 and other factors that are not considered in our model, the model has succeeded quite well in predicting the state of the outbreak one year ahead. For example, even for Mexico, where our prediction of the magnitude is relatively worse than the other places, the model still correctly predicts that the outbreak is small in 2021.

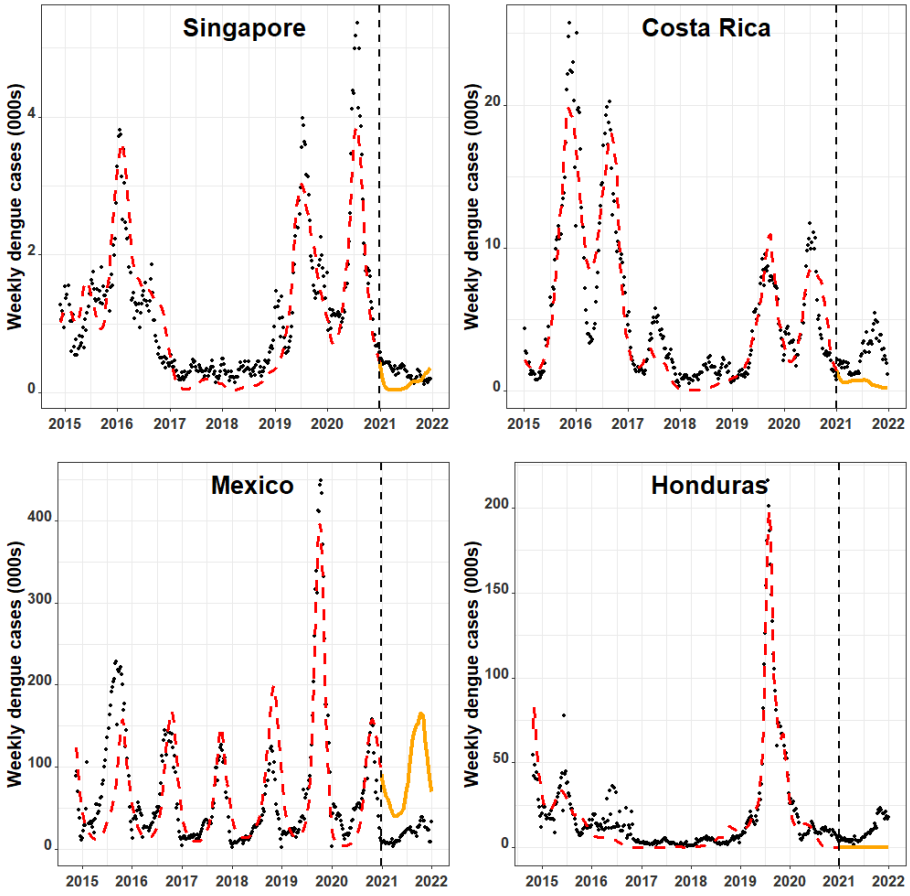

Figure 5: **Fitted dynamics of estimated models based on data from 1/1/2015 to 12/30/2020, and predicted dynamics for 2021. In each panel, the black dots are the observed weekly dengue cases. The red dashed lines are the simulated dynamics and orange lines are the predictions for 2021.**

7 Bifurcation analysis of temperature on dengue dynamics

We have done more simulations by considering two scenarios for the models in Fig. 3 in the main context with Fig. 3(A) showing that higher temperatures postponed the peak of the dengue epidemics. The first simulation is to change the daily temperature by adding a constant d,

$$Temp_t = d + Temp_t^0, \tag{3}$$

and the second by multiplying the daily temperature by c while keeping the lowest temperate in a year unchanged,

$$Temp_t = c \times (Temp_t^0 - m) + m, \tag{4}$$

where Temp_t^0 is the current temperature on t-th day of a year in Singapore, and $m = \min(\text{Temp}_t^0, \text{t}=1, 2, ..., 365)$. For each case, we perform a bifurcation analysis of the peak time of the year and the corresponding number of cases, as shown in Fig. 6, in which the dynamics become more chaotic as the temperature increases.

But we do not know why the peak time of the year is postponed when temperatures increase. Intuitively, when temperatures are higher, the dynamics become more chaotic because more of the year is conducive to transmission, leading to outbreaks at any given time. Interestingly, these increasingly chaotic dynamics are observed in real-world dengue transmission, as shown in Fig. 7.

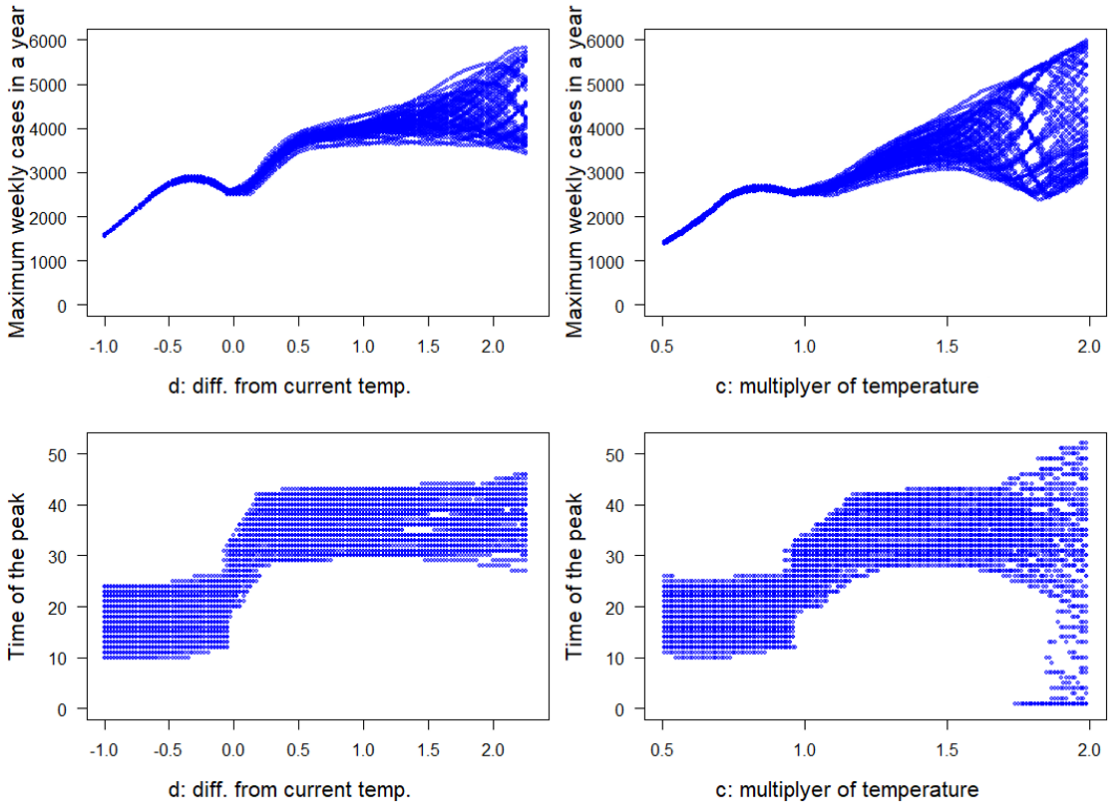

Figure 6: **Bifurcation analysis of the fitted dynamics with different temperature.**

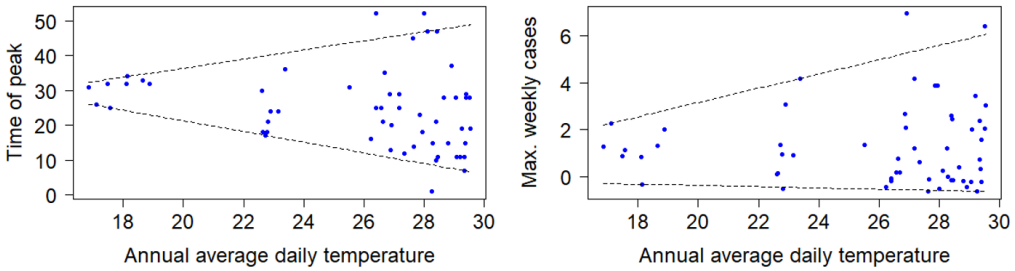

Figure 7: **Observed time of peak and maximum number of cases in a year in Singapore, Bangkok, Changimai, Chonburi, Nakhon Sawan, Costa Rica, Bolivia, Honduras and Mexico, the weekly cases are scaled by the average in the corresponding place. The two dashed lines are the 5% and 95% quantile regressions respectively.**

8 Effect of diurnal temperature range

Some studies [8, 9] also noted that the diurnal temperature range (DTR) affects some of significant factors underlying DENV transmission. Due to data availability, we include DTR into the ETSIR(S) models of three regions, namely Singapore, Bangkok and Costa Rica with mean DTR 6.16°C, 8.41°C and 10.73°C respectively. Following the discussions in section **Quantifying the effect of weather conditions** in the main context, a general ETSIR(S) model with DTR is:

$$E(I_t) = \{c_0 + c_I \times \sum_{k=1}^{K_I} I_{t-k} + \mathrm{g}_P(\sum_{k=1}^{K_P} P_{t-k}/K_P) + \mathrm{g}_T(\sum_{k=1}^{K_T} T_{t-k}/K_T) + c_{DTR} \times \sum_{k=1}^{K_{DTR}} DTR_{t-k}/K_{DTR}\} \times I_{t-1}. \quad (5)$$

where DTR_t is diurnal temperature range at time t. The estimated parameters in the models are listed in Table 4 and the estimated coefficients of DTR are -3.12×10^{-4}, -2.40×10^{-2} and -4.30×10^{-2} with p-values 0.14, 0.086 and 0.02 respectively, implying hindering effect on the transmission that becomes more significant as the average DTRs increases

(from low to high), in line with the conclusion in [8, 9].

Table 4: **Estimated parameters for ETSIR(S) with DTR for Singapore, Bangkok and Costa Rica. [1]Values on top are the regression coefficients. [2]Values in the bracket are the corresponding p-values based on re-sample method (3).**

	Countries		
Coefficients	Singapore	Bangkok	Costa Rica
c_0	-2.80 (5.00×10^{-4})	-1.51×10^{-1} (0)	-2.45 (1.00×10^{-3})
c_I	-1.55×10^{-6} (0)	-9.07×10^{-6} (6.50×10^{-2})	-3.04×10^{-7} (0)
c_P	2.32×10^{-2} (1.50×10^{-3})	1.00×10^{-1} (0)	1.13×10^{-1} (9.15×10^{-2})
c'_P	-1.15×10^{-2} (1.60×10^{-2})	-1.70×10^{-1} (8.50×10^{-2})	-1.87×10^{-1} (2.00×10^{-2})
c_T	1.23×10^{-1} (8.50×10^{-3})	2.70×10^{-2} (5.00×10^{-4})	1.39×10^{-1} (0)
c'_T	-1.39×10^{-1} (1.00×10^{-3})	-9.80×10^{-3} (2.92×10^{-1})	-8.21×10^{-2} (4.50×10^{-2})
c_{DTR}	-3.12×10^{-4} (1.44×10^{-1})	-2.40×10^{-2} (8.60×10^{-2})	-4.30×10^{-2} (1.90×10^{-2})

9 Remarks on GAI index

The weekly GAI index was collected in Singapore from January 2014 to September 2016 [1]. The gravitrap contained a hay infusion solution, which acts as a lure for gravid female *Aedes* mosquitoes. Gravitrap *aegypti* index (GAI), derived from the gravitrap surveillance data, was defined as the mean number of female adult *Ae. aegypti* caught per functional gravitrap and can be written as:

$$GAI = \frac{\text{the number of female adult } \textit{Ae. aegypti}}{\text{the number of functional Gravitrap}}. \tag{6}$$

10 Estimation details using GAI data

For the effect of temperature on GAI index discussed in section **Roles of weather conditions in dengue vector** in the main context, the dependence of GAI on the temperature

is modelled as follows:

$$E(GAI_t|T_{t-i}, i = 1, 2, ...) = f_T(\sum_{i=1}^{K_T} T_{t-i}/K_T),$$

where f_T denotes regression function. Based on the smallest Akaike information criterion (AIC), with K_T=120, the analysis in the main context suggests a significant influence of temperature on the GAI (with p-value < 0.0001 based on spline-regression [10]).

Next, we divide the data into three groups according to the GAI index to remove the effect of the *Ae. aegypti* abundance. As shown in Fig. 8, *Ae. aegypti* abundance doesn't have significant effect on dengue incidences in each group with p-values 0.3270, 0.2580 and 0.3850 respectively. For each GAI group, we again use spline-regression to estimate the effect of cumulative temperature on dengue incidences.

$$E(I_t|T_{t-i}, i = 1, 2, ...) = h_T(\sum_{i=1}^{K_T} T_{t-i}/K_T),$$

where h_T denotes regression function. With $K_T = 60$, the analysis in the main context suggests significant effects of temperature on dengue incidences with p-values 0.0027, 0.0002 and 0.0327 respectively after removing the effect of the *Ae. aegypti* abundance for their spline regressions.

Similar to the temperature, the effect of precipitation on *Ae. aegypti* abundance can be written as:

$$E(GAI_t|P_{t-i}, i = 1, 2, ...) = f_P(\sum_{i=1}^{K_P} P_{t-i}/K_P).$$

With K_P=21, the precipitation also has significant nonlinear effect on *Ae. aegypti* abundance as shwon in Fig. 9(A) with p-value < 0.001. After removing the effect of the *Ae. aegypti* abundance, precipitation still has significant nonlinear effect on dengue incidences in the low GAI group with p-value < 0.001 as shown in Fig. 9(B), while the p-values for the medium and high groups are 0.150 and 0.397 respectively, indicating that the effect of precipitation is less than that of temperature.

Because of the small data size, we are unable to analyse the temperature and precipitation simultaneously.

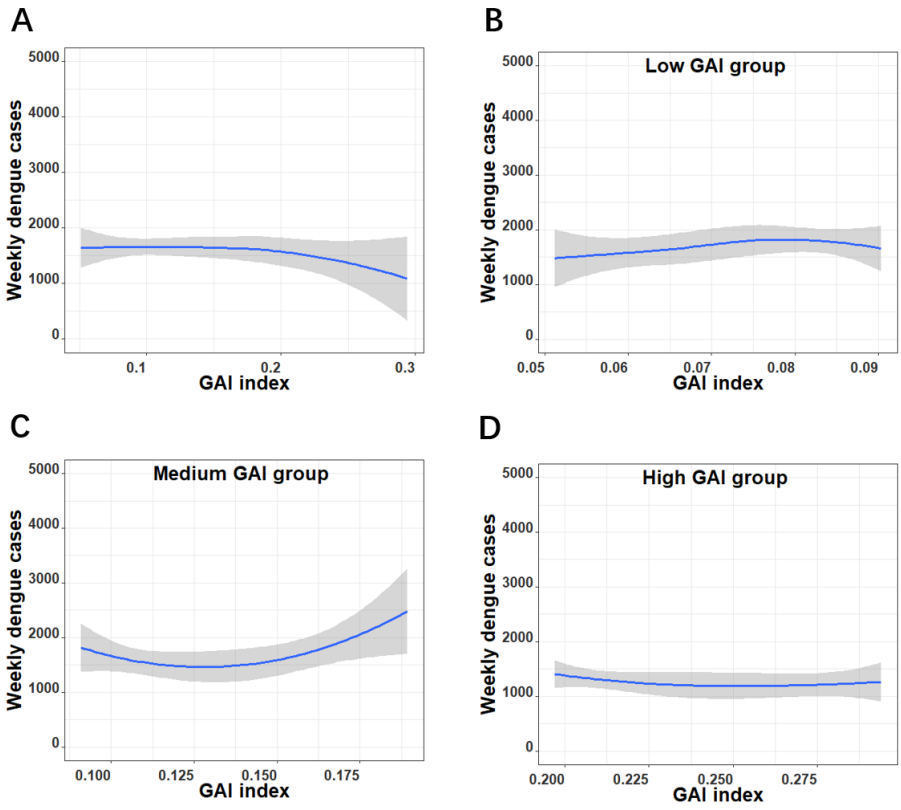

Figure 8: **Effect of GAI index on dengue incidences as discussed in Section 10. [A]Effect of overall GAI index on dengue incidences. [B]Effect of GAI index on dengue incidences for low GAI group. [C]Effect of GAI index on dengue incidences for medium GAI group. [D]Effect of GAI index on dengue incidences for high GAI group.**

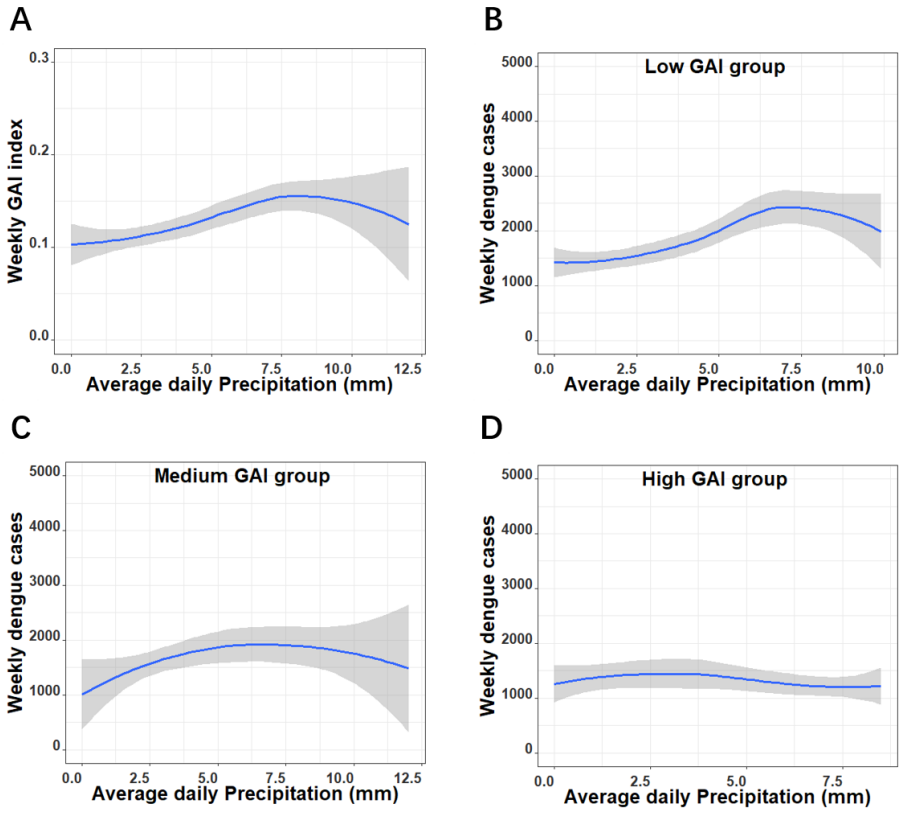

Figure 9: **Effect of precipitation on GAI index and the effect of precipitation on dengue incidences with different groups of GAI index as discussed in Section 10. [A]Effect of precipitation on GAI index. [B]Effect of precipitation on dengue incidences for low GAI group. [C]Effect of precipitation on dengue incidences for medium GAI group. [D]Effect of precipitation on dengue incidences for high GAI group.**

References

[1] Ong J, Chong CS, Yap G, Lee C, Abdul Razak MA, Chiang S, et al. Gravitrap deployment for adult *Aedes aegypti* surveillance and its impact on dengue cases. PLOS Neglected Tropical Diseases. 2020 08;14:e0008528.

[2] Tan LK, Low SL, Sun H, Shi Y, Liu L, Lam S, et al. Force of infection and true infection rate of dengue in Singapore: implications for dengue control and manage-

ment. American Journal of Epidemiology. 2019 05;188(8):1529-38. Available from: https://doi.org/10.1093/aje/kwz110.

[3] Wichmann O, Yoon IK, Vong S, Limkittikul K, Gibbons R, Mammen M, et al. Dengue in Thailand and Cambodia: an assessment of the degree of underrecognized disease burden based on reported cases. PLOS Neglected Tropical Diseases. 2011 03;5:e996.

[4] Sarti E, L'Azou M, Mercado M, Kuri P, Siqueira JB, Solis E, et al. A comparative study on active and passive epidemiological surveillance for dengue in five countries of Latin America. International Journal of Infectious Diseases. 2016 March;44:44—49. Available from: https://doi.org/10.1016/j.ijid.2016.01.015.

[5] Efron B, Tibshirani RJ. An Introduction to the Bootstrap. Chapman and Hall/CRC; 1993.

[6] Wilder-Smith A, Earnest A, Tan S, Ooi E, Gubler D. Lack of association of dengue activity with haze. Epidemiology and Infection. 2010 04;138:962-7.

[7] Thiruchelvam L, Dass S, Zaki R, Yahya A, Asirvadam V. Correlation analysis of air pollutant index levels and dengue cases across five different zones in Selangor, Malaysia. Geospatial Health. 2018 05;13:613.

[8] Lambrechts L, Paaijmans KP, Fansiri T, Carrington LB, Kramer LD, Thomas MB, et al. Impact of daily temperature fluctuations on dengue virus transmission by *Aedes aegypti*. Proceedings of the National Academy of Sciences. 2011;108(18):7460-5. Available from: https://www.pnas.org/doi/abs/10.1073/pnas.1101377108.

[9] Carrington L, Seifert S, Armijos V, Lambrechts L, Scott T. Reduction of *Aedes aegypti* vector competence for dengue virus under large temperature fluctuations. The American journal of tropical medicine and hygiene. 2013 02;88:689-97.

[10] Hastie TJ, Tibshirani RJ. Generalized additive models. Chapman & Hall/CRC Monographs on Statistics & Applied Probability. Taylor & Francis; 1990. Available from:

https://books.google.com.sg/books?id=qa29r1Ze1coC.